Visakhapatnam Chapter

Proceedings of Indian Geotechnical Conference 2020
December 17-19, 2020, Andhra University, Visakhapatnam

Some Aspects of Seismic Soil–Structure Interaction of Lifeline Structures

M. N. Viladkar

Professor & Emeritus Fellow (Retd.),
Department of Civil Engineering., IIT Roorkee, Roorkee, India
mnviladkar50@gmail.com

Abstract. Historically, underground structures were considered to be less vulnerable to earthquakes. However, some of the recent earthquakes have demonstrated that underground structures too can suffer severe damages, especially when these are located in the vicinity of causative faults. Strong ground shaking can cause loss of strength in saturated cohesion less soils resulting into *liquefaction*. Liquefaction can cause the ground surrounding the tunnels to shift, with potentially severe consequences. An attempt has been made in this paper to study various analysis and design considerations of underground lifeline structures and then look in to the aspects of stability of metro underground tunnels of Delhi city on basis of response spectra compatible time histories of 1999 Chamoli earthquake of Uttarakhand, actual three dimensional analyses, and some liquefaction studies.

Keywords: Response Spectra Compatible Time History, Peak Ground Acceleration, Liquefaction.

1 Introduction

Lifeline Structures, like tunnels used in metropolitan cities for mass rapid transit system, water conductor systems of hydro power projects, roadway / railway tunnels in hilly areas, structures like national highways particularly in hill areas, gas transportation pipelines, etc., are the strategic elements in transportation and utility networks. Historically, such underground structures were considered to be less vulnerable to earthquakes as compared to structures built on the ground surface. However, underground structures cannot be treated as completely exempt to the effects of ground shaking, as was demonstrated by the 1995 Kobe earthquake in Japan, 1999 Chi-Chi earthquake in Taiwan, and 2004 Niigata earthquake again in Japan, where several underground structures suffered severe damages [15]. The growing need in recent years to enlarge these transportation networks is the cause of a renewed interest for studying the vulnerability of such underground facilities to seismic loading. The importance of these structures makes their vulnerability to earthquakes a very sensitive issue. A large earthquake would not only cause the direct but also the indirect damages resulting into not only the potential loss of human lives but also into damage to many other infrastructures. This can finally result into severe economic losses, especially in view of the time required to restore the functionality of the network. In order to reduce the potential loss of serviceability of these structures, it is essential to reduce the possible risk associated and the effects of damage.

A careful review of the seismic damages suffered by underground facilities shows that most tunnels were located in the vicinity of causative faults. The characteristics of ground motion in the vicinity of the source can be significantly different from that of the far-field. The ground motion close to an active fault may be characterized by strong, coherent (narrow band) long period pulses and is severely affected by the rupture mechanism, the direction of rupture propagation relative to the site, and the possible permanent ground displacements resulting from the fault slip. One of the first compilations of data on damage to 71 tunnels in rock due to earthquake shaking [11] and comparison of their behavior with estimated PGAs and PGVs concluded that- i) Collapse of tunnels due to ground shaking occurs only under extreme conditions, ii) damage did not occur so long as the PGA was lower than 0.19 g and/or PGV was lower than 0.2 m/s, iii) minor to moderate damage occurred when PGA went up to 0.5 g and PGVs up to 0.9 m/s, iv) moderate to heavy damage occurred when the PGA was larger than 0.5 g, and v) tunnel collapse occurred only when it was associated with movement of an intersecting fault.

Another important aspect of the problem is that strong ground shaking can cause loss of strength in saturated cohesion less soils which results into phenomenon of liquefaction. The consequences of liquefaction may include bearing capacity failure giving rise to sinking of a structure, lateral spreading, and the slope instability. Slope instability at portals and fault displacements can cause at times catastrophic damage. Liquefaction can cause the ground surrounding the tunnels to shift, with potentially severe consequences. It can lead to collapse of multiple underground structures (collapse of a subway station in Kobe, Japan during the 1995 deadly Great Hanshin earthquake). Ground movements associated with landslides can cause damage to a highway facility, generate other types of secondary impacts, and rupture the water or gas supply pipelines. Fire or explosions have historically been a major source of damage following the earthquakes. Rupture of a gas pipe line and electric power supply lines is often the cause of dramatic explosions and fires. Major fire that broke out as a result of the 1994 Northridge earthquake in USA was due to the rupture of a gas pipe).

The seismic analysis of underground structures is therefore a complex task, since it involves the interaction with several disciplines including structural geology, seismo-tectonics, engineering seismology, soil and rock dynamics, and structural dynamics. This area has by far remained somewhat neglected primarily because of the conventional notion that underground structures are not sensitive to earthquakes. As a consequence, engineers often omit the evaluation of structural performance of tunnels under seismic conditions at the design stage.

2 Design Considerations

In case of an underground project which is located at a relatively shallow depth in an urban area, design and construction will probably be more demanding due to interaction between the underground project and the overlying pre-existing

structure(s) such as buildings, bridges, etc. This interaction may be more complicated, since the "effect of local site conditions" can play a major role. This was realized during the 1995 Kobe earthquake in Japan (damage to bridges) and 1999 Chi-Chi earthquake in Taiwan (extensive failures in tunnels and buried gas pipelines).

Seismic response of tunnels and underground structures is considerably different from that of above-ground facilities because the overall mass of the structure is usually small as compared to the mass of the surrounding soil/rock and the overall confinement provides high level of radiation damping. Therefore, seismic response of an underground structure is basically controlled by the response of the surrounding ground and by the imposed ground deformation and not by the inertial characteristics of the structure itself, because the response to such an event is substantially dependent on the induced ground deformation.

Selection of realistic ground motion of an earthquake is therefore very important for the seismic analysis and design of underground structures. The time history of an earthquake should therefore be such that it can match the expected earthquake in that particular zone or at the site in question, and hence it necessitates generation of response spectra compatible time history.

In majority of the cases, it may not be possible to have strong motion records at a given site. Even if such records are available, there is no basis to expect that a future earthquake might generate the same or similar ground motion. The selected time history should adequately represent the ground motion that can be expected at the site, and in particular, the motion that would make the structure respond to the highest damage potential. It is therefore essential that for predicting the earthquake response of a structure, synthetic time histories are generated for the specific sites. However, there are several uncertainties in this process, and to overcome these; decisions are required to be taken in a scientific and purposeful manner. Some of the issues involved in the process of generation of site specific synthetic accelerograms are - i) shape of design response spectra, ii) zero period acceleration (ZPA), iii) duration of record, iv) strong motion and decay time (envelop function of time history), v) phase characteristic of the record, vi) number of zero crossings, and vii) realistic derived velocity and displacement history, etc.

To generate site specific time histories, first a target response spectra and duration of time history for the site are estimated. These are generally based on specific site characteristics and size as well as the distance of site from the epicenter of the postulated earthquake. Subsequently, a spectrum compatible time history is generated. Theoretically there can be infinite number of compatible time histories for a given response spectra and therefore, question often arises as to which time history has the maximum damage potential and has the near-fault effects. There is therefore a need to have a spectrum compatible time history which has the near-fault effects. Several time histories recorded very close to the epicenter show distinguishable velocity pulse (commonly called as "fling") of significant duration, which implies that very large energy is concentrated in that duration of the pulse. It is therefore a matter of research whether such time histories are more damaging than the other time histories, which do not have such a velocity pulse. But surely, a need arises to generate spectrum compatible time histories, which have a velocity pulse. It has been found that while

generating spectrum compatible time history, if one uses the phase of a recorded time history which has a distinguishable velocity pulse (instead of a random phase as is the general practice), then the resulting spectrum compatible time history may also have a similar velocity pulse [21].

3 Generation of Response Spectra Compatible Time History for Delhi City

Various authors, namely ([1], [13], [30], [23], [7], [14], [28], [10], [29], [2], [33], [39], [43], [6], [12], [19], [31], [32]) have also studied the influence of response spectra compatible time history.

3.1 Generation of target response spectra

As a first step, target response spectra of Delhi city have been obtained. Since Delhi city is in seismic zone-IV, target response spectra for this zone are to be generated. Target response spectra have been generated according to [18] for Design Basis Earthquake (DBE) and Maximum Considered Earthquake (MCE). These spectra were generated for different damping ratios of Delhi silt. Plot of spectral acceleration, Sa (in terms of g) with the time period T (sec) has been presented in Figs. 1 and 2 for MCE and DBE respectively. Maxima values of spectral acceleration considering MCE are 0.6g, 0.48g and 0.42 corresponding to 5%, 10% and 15% damping respectively (Fig. 1); whereas for DBE, these values are found to be half of those for MCE (Fig. 2).

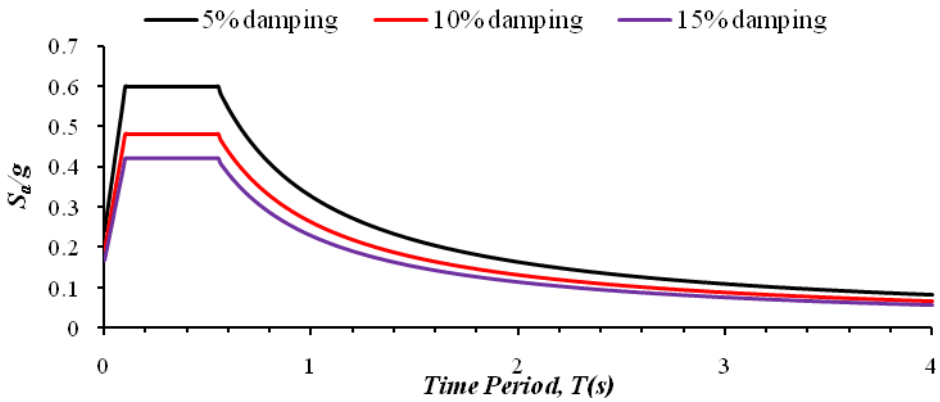

Fig. 1. Response spectra for zone IV (medium soil) for different damping ratios, and for Maximum Considered Earthquake (MCE) [18].

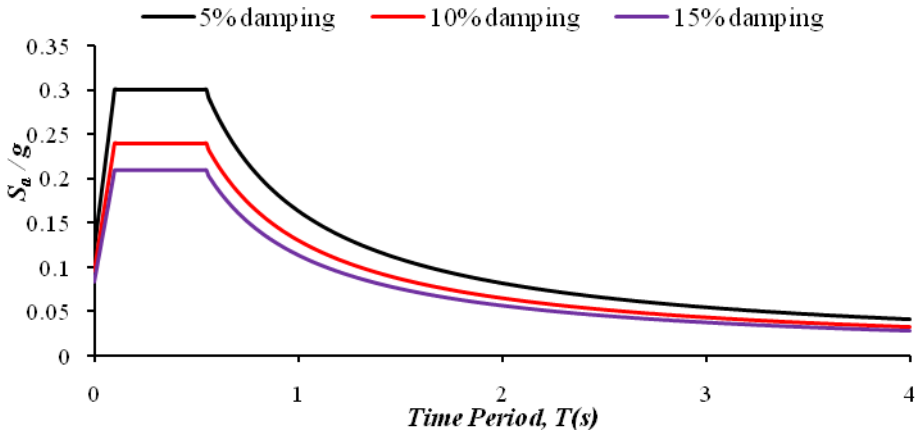

Fig. 2. Response spectra for zone IV (medium soil) for different damping ratios, and for Design Based Earthquake (DBE) [18].

3.2 Selection of adequate Time-History

Since no major earthquake has occurred in Delhi city, therefore 1999 Chamoli, earthquake of lower Himalaya has been chosen for analysis (PGA for this earthquake is larger than that for 1991 Uttarkashi earthquake). The magnitude of the earthquake was 6.8 on Richter scale. Time history record of the horizontal component of this earthquake after applying the base line correction is presented in Fig. 3 [18]. Horizontal acceleration is denoted by Ax. Peak ground acceleration (PGA) of this earthquake was 3.53 m/sec2 equivalent to 0.359 of g.

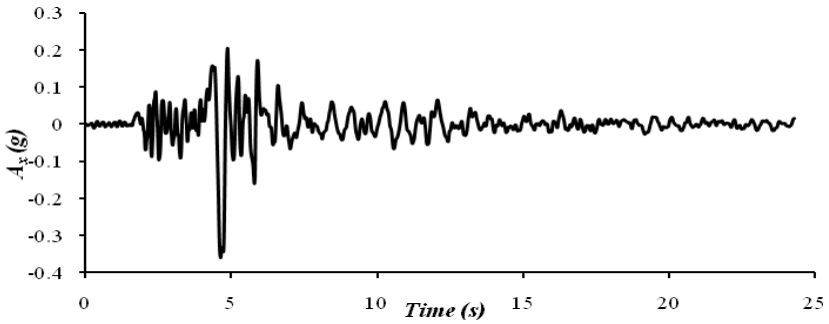

Fig. 3. Horizontal acceleration (Ax) - time history of 1999 Chamoli earthquake [31].

3.3 Response spectra compatible time-history

1999 Chamoli earthquake occurred in Chamoli district of the Garhwal Himalaya which exists in zone-V of earthquake zoning map of India (IS: 1893: Part 1, 2002). However, Delhi falls in zone- IV in this map. Therefore artificial time history has to

be generated for zone-IV. Taking the magnitude of acceleration from target spectra (Figs. 1 and 2) and phase from given input history (Fig. 3), response spectra compatible time histories have been generated using Spec3, WAVGEN and SiesmoMatch softwares [31]. Figures 4, 5, and 6 show respectively the modified time-histories considering target response spectra of MCE by Spec3, Wavgen and SeismoMatch softwares respectively. Similarly, modified time-histories were also generated considering the target response spectra of DBE by Spec3, Wavgen and SeismoMatch softwares respectively. The phase and time interval of modified time history are same as the actual earthquake [33].

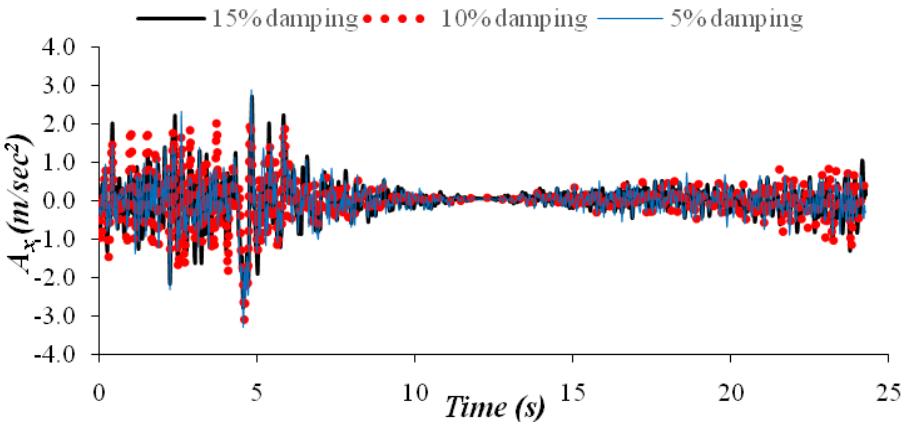

Fig. 4. Response spectra compatible time-history for MCE response spectra by Spec3 [31].

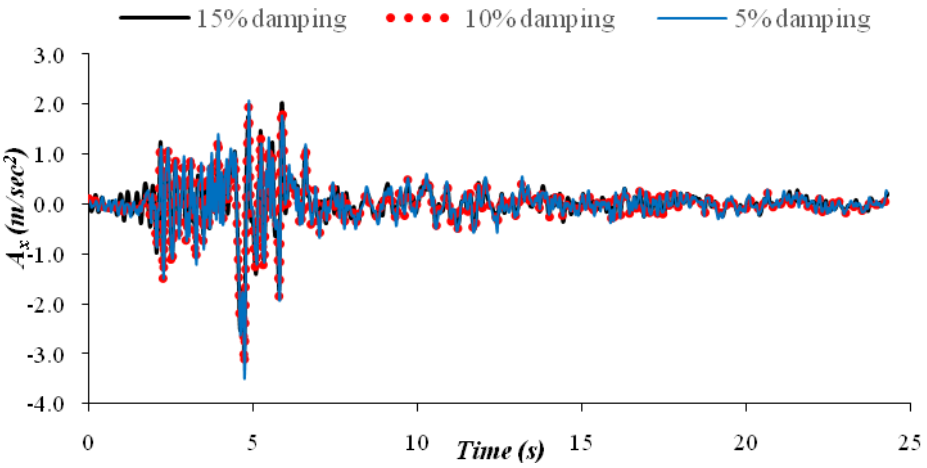

Fig. 5. Response spectra compatible time-history for MCE response spectra by WAVGEN [31].

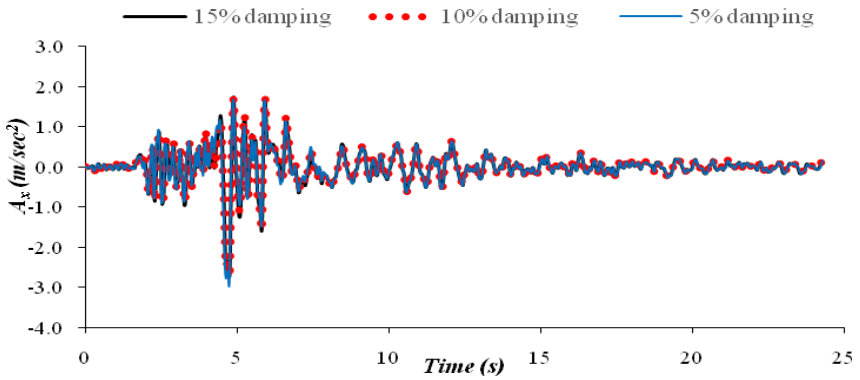

Fig. 6. Response spectra compatible time-history for MCE response spectra by SeismoMatch [31].

The maximum values of PGA obtained from different software packages have also been summarized in Table 1 for the sake of comparison. It can be seen that PGA values of the artificial time histories obtained by Spec3, Wavegen and SeismoMatch increase with reduction in damping. It can be noticed from Fig. 7 that the trend of artificial time history generated by SeismoMatch is quite similar to the actual earthquake (Fig. 3) except for the value of peak ground acceleration.

Table 1. Comparison of PGA values obtained from different software packages for different damping ratios [31].

Software	PGA (m/sec^2)					
	MCE			DBE		
	15% damping	10% damping	5% damping	15% damping	10% damping	5% damping
Spec3	2.78	3.11	3.29	1.39	1.55	1.64
Wavgen	2.97	3.23	3.50	1.49	1.62	1.75
SeismoMatch	2.73	2.77	2.97	1.65	1.66	1.76

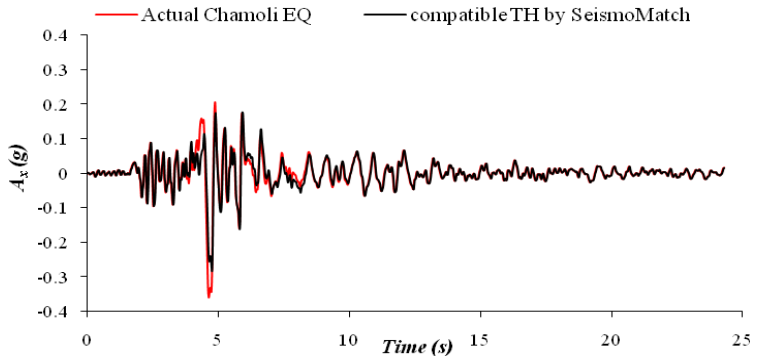

Fig. 7. Actual 1999 Chamoli earthquake acceleration-time history and response spectra compatible time history of MCE (obtained by SeimoMatch for 10% damping) [31].

4 Case History of Delhi Metro Underground Tunnels

In this section, a typical section of DMRC (Delhi Metro Rail Corporation) tunnels constructed in Connaught Place between Rajiv Square and Patel Square has been considered for analysis. This section of tunnels, referenced as line-B6, is situated on the Yellow line and was constructed in Phase-I of the work of DMRC. The diameter of DMRC tunnel in Connaught place is 6.26 m with an overburden depth of 16.87 m. Reinforced Concrete (RC) liners, with a thickness of 0.28 m, have been used as a permanent support system. Elastic modulus of RC liners, E_c is 3.16 x 10^7 kPa and the Poisson's ratio is 0.15. The problem is summarized in Fig. 8.

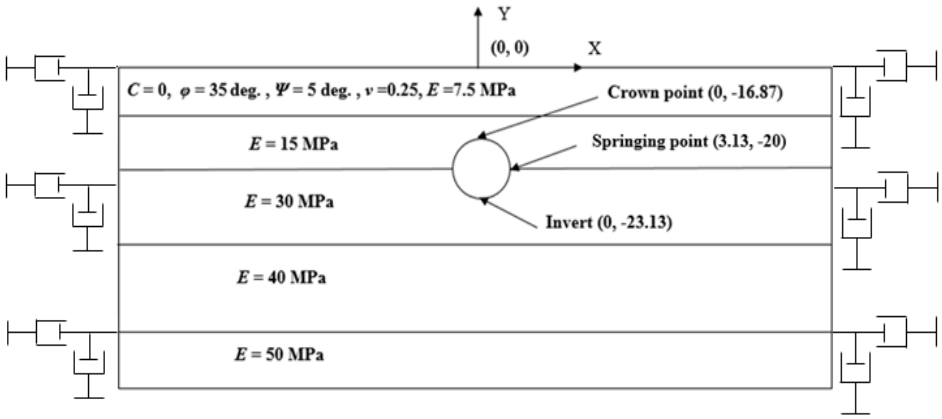

Fig. 8. Geometry of soil–tunnel system.

DMRC tunnels have been excavated through alluvium deposits, generally known as Delhi silt. For the present study, engineering properties of alluvium have been adopted from [36, 44] and the variation of elastic modulus of Delhi Silt with depth has been summarized in Table 2. In-situ unit weight, γ_{bulk} and saturated unit weight, γ_{sat} of Delhi silt were found to be 18 kN/m^3 and 20 kN/m^3 , respectively. No water table was encountered during tunnel excavation. Thickness of each soil was 10m except layer 3 which has 15m thickness.

Table 2. Variation of elastic modulus of Delhi Silt with depth [36].

Depth (m)	Thickness (m)	Elastic modulus (kPa)
0-10	10	7500
10-20	10	15000
20-35	15	30000
35-50	15	40000
50-60	10	50000

Two dimensional plane strain finite element analysis has been carried out with rectangular domain, 200 m x 60 m, using 6-noded triangular elements for the soil mass. Elasto-plastic behavior of soil mass was simulated by Mohr-Coulomb yield criterion. The RC liners of the tunnel were modeled through 32 plate bending elements. Linear elastic behavior of RC liners was considered in the analysis. Damping in RC liner has been taken as 2%. No-slip condition (perfect bond between RC liners and the surrounding soil mass) was assumed between the tunnel and surrounding soil. For static response, nodes along vertical boundaries were restrained in X direction and were free to move in Y direction whereas the bottom boundary was restrained in both x and y directions. For dynamic analysis, viscous absorbent boundary, proposed earlier by [25], was used to represent displacement condition along both vertical boundaries. No boundary condition was applied along the horizontal base boundary and earthquake was applied at the base of the model along this boundary. Actual 1999 Chamoli earthquake and all response spectra compatible time-histories corresponding to 10% damping have been considered for analysis. The seismic response of soil-tunnel system has been plotted for different time histories and the response has been presented here in the form of induced acceleration, horizontal displacements in the system, and forces in RC liners.

4.1 Displacement response

Values of maximum horizontal displacements induced in soil-tunnel system during the earthquake are presented in Table 3 for different response spectra compatible time histories as well as for the actual earthquake. These values are presented for ground-surface, crown, invert and the springing points of tunnel. It can be noticed from Table 3 that Spec3 and Wavgen algorithms significantly overestimate the horizontal displacements whereas SeismoMatch predicts horizontal displacements which are comparable for both MCE and DBE and are also comparable to those obtained for the

Table 3. Maximum horizontal displacements of soil-tunnel system during earthquake for different response spectra compatible time histories [31].

Location	Maximum horizontal displacement U_x (mm)						
	1999 Chamoli EQ, Actual	Response spectra compatible time-history (MCE)			Response spectra compatible time-history (DBE)		
		Spec3	Wavgen	Seismo-Match	Spec3	Wavgen	Seismo-Match
Ground surface (A)	264	2975	1094	209	1490	532	205
Crown (B)	154	2973	1502	185	1480	535	174
Invert (C)	151	2973	1485	180	1480	536	165
Springing Point (1)	119	2013	1133	149	1522	583	136
Springing point (2)	185	2059	1067	216	996	516	203

horizontal component of actual 1999 Chamoli, earthquake. It can therefore be concluded that time history generated by SeismoMatch gives more reliable results compared to those given by Spec3 and Wavgen algorithms. Similarly values of maximum vertical displacements induced in soil-tunnel system during the earthquake are presented in Table 4 for different response spectra compatible time histories as well as the actual earthquake. It can be seen that vertical displacements at all critical locations show a very good mutual comparison for all time histories of earthquake. It can as well be noticed that vertical displacement is maximum at the crown point of tunnel. softwares respectively. Similarly, modified time-histories were also generated considering the target response spectra of DBE by Spec3, Wavgen and SeismoMatch softwares respectively. The phase and time interval of modified time history are same as the actual earthquake.

Table 4. Maximum vertical displacements of soil-tunnel system during earthquake for different response spectra compatible time histories [31].

Location	Maximum vertical displacement U_y (mm)						
	Actual 1999 Chamoli earthquake	Response spectra compatible time-history (MCE)			Response spectra compatible time-history (DBE)		
		Spec3	Wavgen	Seismo-Match	Spec3	Wavgen	Seismo-Match
Ground surface	35	35	31	31	30	29	29
Crown	77	79	76	76	76	75	74
Invert	50	48	49	49	48	49	49
Springing point (1)	20	18	18	18	16	16	15
Springing point (2)	14	20	16	15	16	15	14

4.2 Forces in RC liners

Values of axial thrust (T), shear forces (V), and bending moment (M) induced in RC liners are also presented in Table 5 for different time histories. As per the sign convention followed in Plaxis, tension is positive and negative sign shows that stresses are compressive in nature. It can be concluded that for acceleration-time history considering MCE target response spectra, Spec3 produces higher values of forces and moments in RC liners as compared to those given by WAVGEN, which in turn are marginally higher than those given by SeismoMatch. This observation is also valid for response spectra time history considering DBE. DBE based response spectra gives values of forces and moments which are on lower side as compared to those given by MCE based response spectra. Moreover, DBE based target response spectra

produces forces and moments in liners which are almost same for all three time histories.

Table 5. Maximum forces in RC liners during earthquake for different time histories [31].

Max. forces in RC liners	Static Analysis	1999 Chamoli Earth-quake, Actual	Response spectra compatible time-history (MCE)			Response spectra compatible time-history (DBE)		
			Spec 3	Wavgen	Seismo-Match	Spec 3	Wavgen	Seismo-Match
T_{max} (kN/m)	-534.98	-627.99	-610.9	-598.62	-595.84	-562.4	-559.76	-561.27
V_{max} (kN/m)	170.20	-211.54	210.80	200.30	196.45	182.30	179.70	172.07
M_{max} (kN-m/m)	-256.83	319.69	327.93	307.56	302.04	273.53	270.34	270.34

4.3 Induced acceleration

Time histories of output acceleration plotted at the crown of tunnel have been presented in Fig. 9 for different applied compatible time histories and for the maximum considered earthquake (MCE) target spectra. It can be observed from Fig. 9 that induced values of acceleration at tunnel crown are respectively 1.64 m/sec^2, 1.43 m/sec^2, and 1.50 m/sec^2, for all the three compatible time histories.

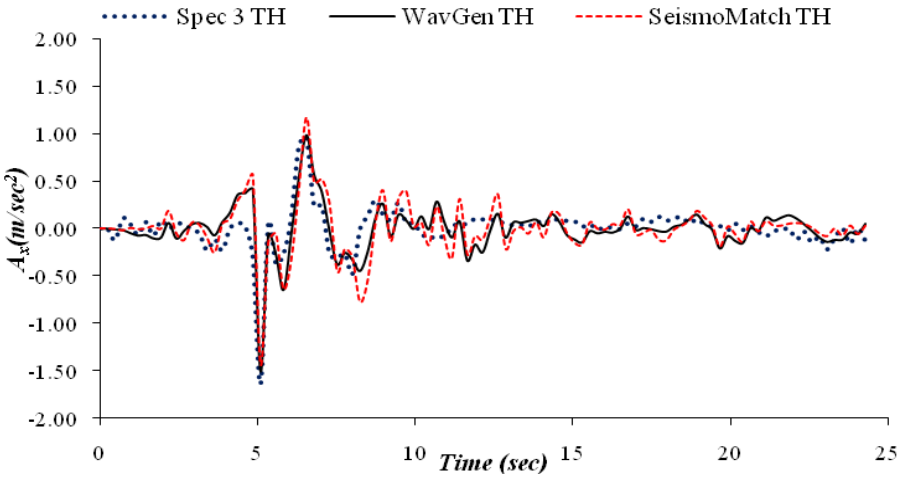

Fig. 9. Horizontal acceleration time history at crown of the tunnel for different time histories (TH), considering MCE [31].

Figure 10 represents the induced acceleration-time history at ground surface for the actual 1999 Chamoli earthquake. It shows that maximum induced acceleration of 2.26 m/sec^2 at the crown point is greater than the corresponding values obtained for the response spectra time histories. It can be therefore be inferred that actual earthquake may overestimate the response of the system and therefore conversion of actual time history in to response spectra time history is very essential.

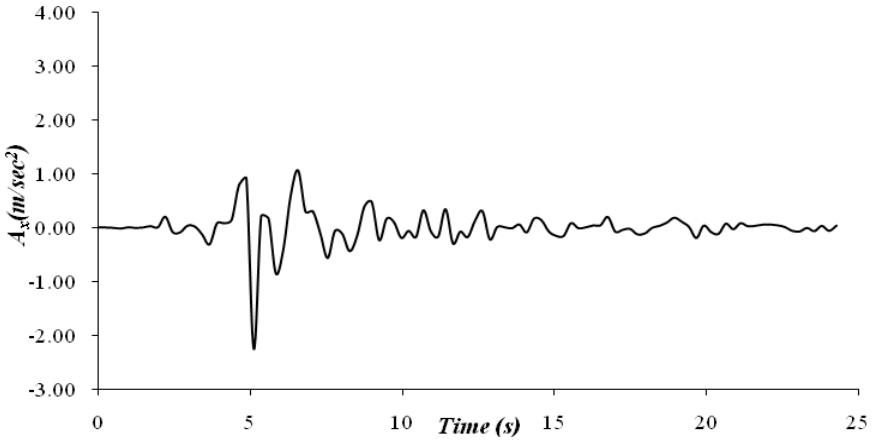

Fig. 10. Horizontal acceleration time history crown of the tunnel for actual 1999 Chamoli earthquake [31].

4.4 Remarks

Based on the above analysis, following concluding remarks can be made:

If earthquake data is not available for a particular site, then earthquake record of another similar site should be taken for analysis. Actual earthquake for another site may overestimate or underestimate the response at the proposed site and therefore conversion of actual time history into response spectra time history is very essential.

All three response spectra compatible time histories yield comparable response in terms of induced acceleration, vertical displacement and forces in RC liners. However, Spec3 and WAVGEN highly overestimate the horizontal displacements as compared to those predicted by SeismoMatch. SeismoMatch based response spectra time history produced results which are quite similar when compared to those for actual earthquake.

5 Significance of Three Dimensional Analysis

Three-dimensional behavior of shallow tunnels under seismic loading by 3D explicit finite difference program (FLAC 3D, [35]). Study presented a three-dimensional nonlinear behavior of a tunnel in soft soil subjected to seismic loading. The originality

of research was about the inclusion of tunnel excavation sequence in the definition of the stress state of soil before the earthquake. For that, tunnel excavation was effected first for generating the initial state of stress in soil; and subsequently, the model was subjected to a seismic excitation. The response included the internal forces induced in the tunnel lining (axial thrust, bending moment and shear force) and the settlement at the ground surface. It was recommended that elastic analysis is not adequate to determine the earthquake induced response of soil-tunnel system. The influence of tunnel installation should be integrated in the model which would lead to a more realistic estimation of the seismic induced thrust force in the tunnel lining and also the surface settlement.

In three-dimensional numerical analysis for the longitudinal seismic response of tunnels under an asynchronous wave input carried out [22], 1D time-domain approach was applied to calculate the free field motion. Based on the numerical approach for the external source wave motion problems, the wave input was determined by applying equivalent nodal force at the truncated boundary, and its accuracy and validity were proved by numerical examples. This wave input method was directly applied to 3-D soil–tunnel structure interaction model to simulate the longitudinal response of tunnels when subjected to asynchronous earthquakes. The results indicated validity of modelling the seismic response of a tunnel with an infinite length as long as the computational model was relatively long in the longitudinal direction. The influence of the angle of incidence and incident direction on the longitudinal seismic response of the tunnel was considered. Several preliminary conclusions were drawn regarding further study and research. Many other authors) have also studied the three dimensional seismic behavior of underground tunnels ([37, 38], [45. 46], [8], [17], [9], and [31, 34]).

5.1 Delhi Metro Tunnel problem

In this study, three dimensional finite element analysis of one of the life line structures i.e. Delhi Metro underground tunnels has been carried out considering response spectra compatible time history of 1999 Chamoli, earthquake. Artificial time histories of all three components of earthquake i.e. horizontal (T), longitudinal (L) and vertical (V) have been generated and used to carry out both linear and non-linear dynamic analyses and the comparison made. Attempt has also been made to compare the dynamic response obtained using three different boundary conditions, namely elementary boundary, absorbent boundary, and the free-field boundary. Moreover, comparison has also been made with the 2-D plane-strain response. All the data od DMRC tunnel remaining the same as that presented in Fig. 10 and Table 2, the only difference is that the depth of overburden here is 12.0m and damping ratio of Delhi silt considered is 15%. No water table was encountered during the tunnel excavation.

The extent of model, after carrying out sensitivity analysis, has been taken as 200 m x 50 m x 60 in X, Y and Z directions respectively. 10-noded tetrahedral elements with an average size of 16.16 m ($< \lambda = 27.65$ m) were considered for modelling of soil domain. Elastic behavior of soil was considered. Segmental RC liners of tunnel were simulated using 6-noded triangular plate bending elements. For RC liners, elastic

behavior was considered. No-slip condition has been assumed between tunnel and the surrounding soil medium. For obtaining static response, boundary displacement conditions were applied along the four vertical surfaces and one bottom surface. Displacements of nodes along four vertical planes were restrained in the direction normal to the planes whereas displacements of all nodes lying on the bottom plane were completely restrained. For dynamic analysis, viscous absorbent boundary (Fig. 8), proposed earlier by [25] was used to represent the displacement condition along both vertical planes.

5.2 Earthquake loadings

All three components i.e. horizontal (T), vertical (V), and longitudinal (L) of the 1999 Chamoli earthquake of the lower Himalaya have been considered for seismic analysis. Response spectra compatible modified time histories of this earthquake were generated for all T, V and L components [31, 34] which are presented in Fig. 11. These histories were applied in turn at the nodes on the bottom plane of the model in X, Z, and Y directions respectively. The components were applied separately (one by one) and not simultaneously. These components have PGA values of 2.713 m/sec^2, 2.044 m/sec^2, and 3.032 m/sec^2 respectively.

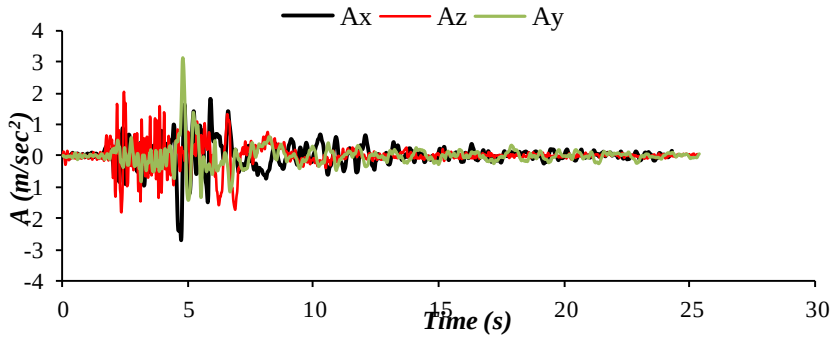

Fig. 11. Response spectra compatible time history for horizontal (A_x), vertical (A_z), and longitudinal (A_y) components of 1999 Chamoli earthquake [31, 34].

5.3 Deformed mesh

Figures 12, 13, and 14 show respectively the deformed mesh due to T, V and L components of 1999 Chamoli earthquake. Values of resultant displacement are of the order of 23.53 mm for T component, 207.00 mm for V component and 193.5 mm for L component of the earthquake. Therefore, maximum value of resultant displacement has been obtained due to the vertical component (V) rather than other two horizontal components of earthquake, namely T and L.

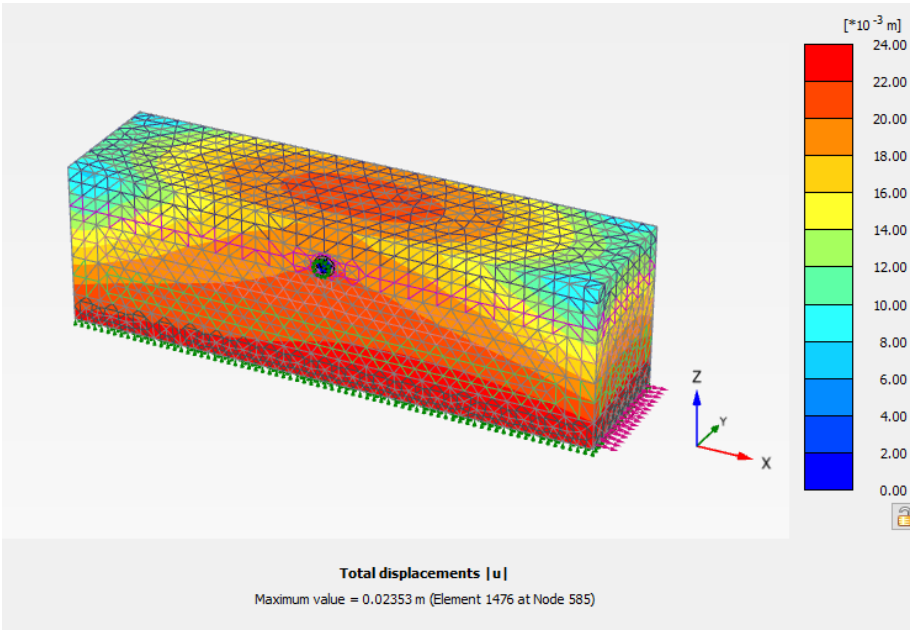

Fig. 12. Deformed mesh due to T-component of earthquake [31, 34].

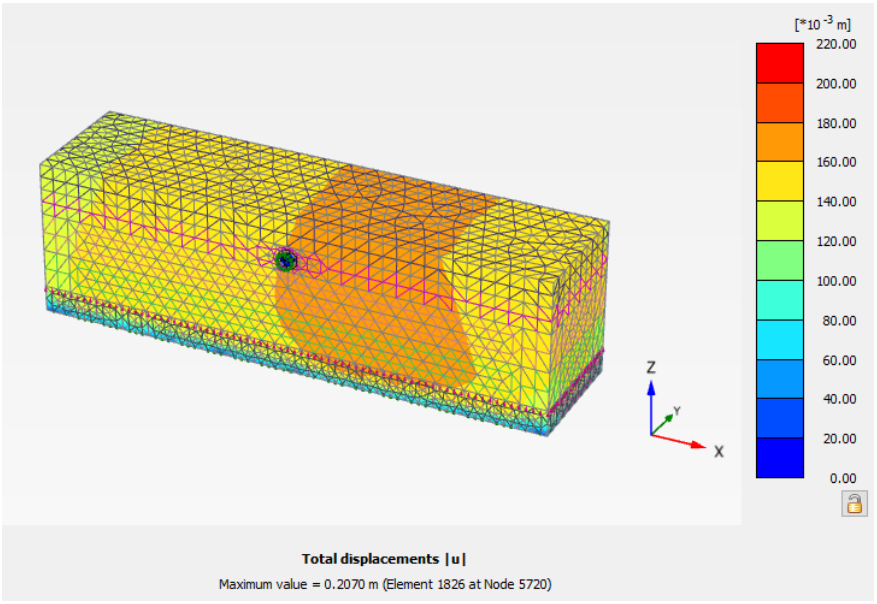

Fig. 13. Deformed mesh due to V-component of earthquake [31, 34].

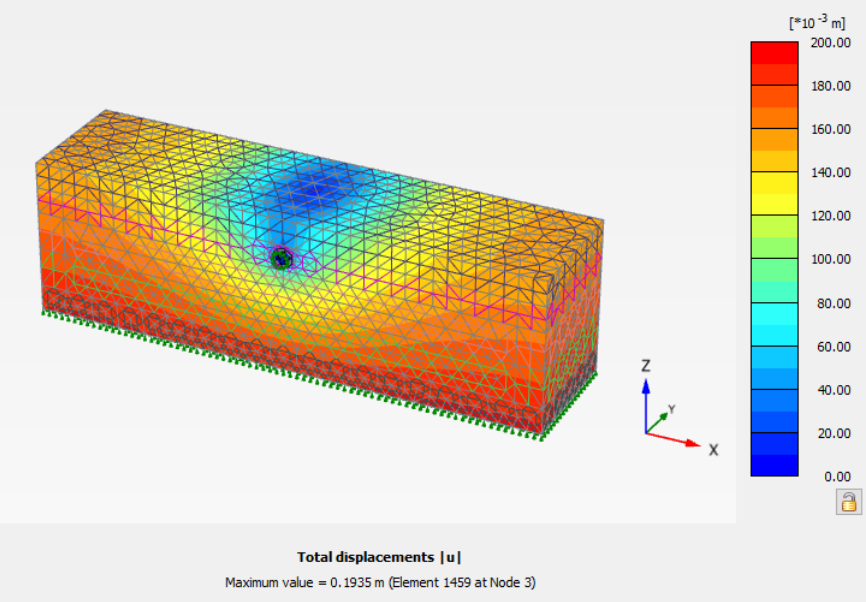

Fig. 14. Deformed mesh due to L-component of earthquake [31, 34].

5.4 Displacements in Soil-Tunnel system

Maximum dynamic displacements in soil-tunnel system after the application of different components of earthquakes have been presented in Table 6. It can be seen that maxima values of horizontal, vertical, and longitudinal displacements, both in soil medium and RC liners of tunnel, occur in respective directions of *T*, *V*, *L* components of earthquake, respectively. For T component, maxima values of horizontal displacement (U_x) predicted are of the order of 23.53 mm in soil medium and 20.50 mm in the tunnel. For V component, maximum values of vertical displacement (U_z) have been found to be of the order 207.00 mm in soil medium and 163.04 mm in the tunnel. Similarly for L component, maximum values of longitudinal displacement (U_y) are 193.5 mm in soil medium and 27.40 mm in tunnel.

Table 6. Maximum dynamic displacements in soil-tunnel system after the earthquake [31,34].

U (*mm*)	Soil medium			Tunnel		
	T comp. of EQ	V comp. of EQ	L comp. of EQ	T comp. of EQ	V comp. of EQ	L comp. of EQ
U_x	23.53	66.72	26.66	20.50	8.626	1.306
U_y	4.74	78.31	193.50	0.024	0.82	27.40
U_z	8.23	207.00	54.76	0.25	163.04	7.84

5.5 Forces in RC liners

Table 7 gives the values of residual forces in RC liners after the earthquake for different components of earthquake. From Table 7, it can be seen that L component of earthquake has produced significantly higher values of forces in RC liners than due to other components of earthquake. However, it has been found that the corresponding axial stress mobilized in the liners is less than 1.0 MPa and hence much less than the permissible tensile strength of concrete. N_1 is the axial force in *Y*-direction, N_2 is the force perpendicular to tunnel axis, (*Y*), Q_{12} is the in-plane shear force in *YZ* plane, Q_{13} is the shear force in *XY* plane, Q_{23} is the shear force in *YZ* plane, M_{11} is bending moment due to bending over the *Z* - axis (around *Z*- axis), M_{22} is bending moment due to bending over the *X*- axis (around *X* axis), and M_{12} is torsional moment according to transverse shear force.

5.6 Induced acceleration

Time histories of induced acceleration have been plotted in Figs. 15, 16 and 17. For T component of earthquake, it can be seen from Fig. 15 that it is the ground surface that

Table 7. Forces in RC liners at the end of earthquake [31, 34].

Forces	δF		
	T component of earthquake	V component of earthquake	L component of earthquake
N_1 *(kN)*	-1.45	51.77	5004.48
N_2 *(kN)*	0.3	6.6	694.545
Q_{12} *(kN)*	4.44	11.95	570.42
Q_{23} *(kN)*	0.12	-2.4	33.32
Q_{13} *(kN)*	0.66	-3.98	9.92
M_{11} *(kN-m)*	-0.016	-0.081	27.71
M_{22} *(kN-m)*	0.12	-3.2	21.17
M_{12} *kN-m)*	0.16	0.218	11.322

-experiences maximum horizontal acceleration of 1.23 m/sec^2 equivalent to 0.125g or 45.3% of the maximum applied horizontal acceleration whereas acceleration level experienced at the tunnel crown is 0.78 m/sec^2 , at tunnel invert, it is 0.95 m/sec^2, and that at the springing points, it is 0.82 m/sec^2. For the V component of earthquake (Fig. 16), it can be observed that it is the ground surface again that experiences maximum horizontal acceleration of 1.65 m/sec^2 equivalent to 0.168g or 80.7% of the maximum applied vertical acceleration whereas acceleration level experienced at the tunnel crown is 1.21 m/sec^2, at tunnel invert, it is 1.04 m/sec^2 and that at the springing points, it is 1.12 m/sec^2. For the L component of earthquake (Fig. 17), It can be noticed that it is the ground surface that experiences maximum longitudinal acceleration of 0.32 m/sec^2 equivalent to 0.032g or 10.5% of the maximum applied horizontal acceleration in Y or L direction whereas acceleration level experienced at

the tunnel crown is 0.23 m/sec^2, at tunnel invert, it is 0.26 m/sec^2 and that at the springing points, it is 0.28 m/sec^2.

5.7 Comparison of 3D analysis with 2D plane strain analysis

3D dynamic response of metro underground metro tunnel has been compared with response predicted from 2D plane-strain analysis. The comparison has been made both for T component and V component of earthquake in terms of horizontal displacement, vertical displacement (Table 8). 3-D analysis leads to overall reduction in horizontal and vertical displacements.

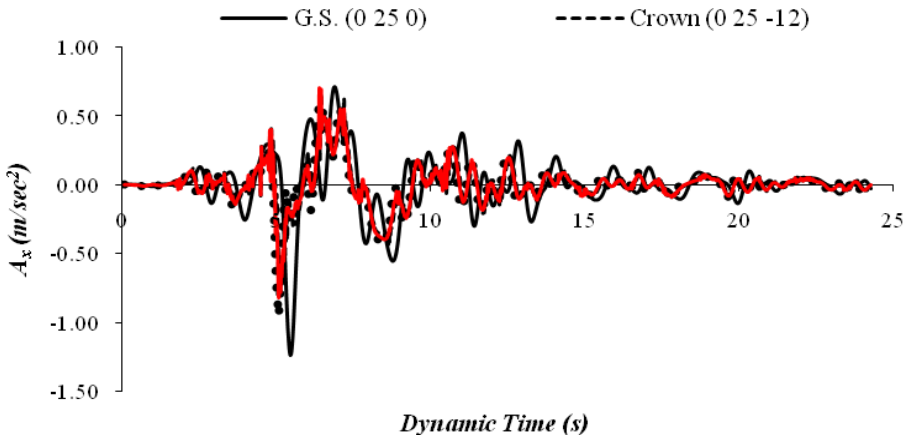

Fig. 15. Time history of horizontal acceleration at the different locations (T component of earthquake) [31,34].

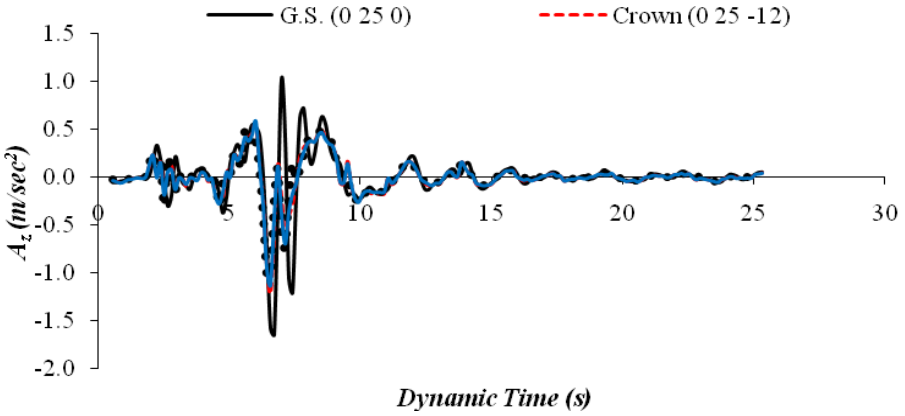

Fig. 16. Time history of vertical acceleration at different locations (V component of earthquake) [31].

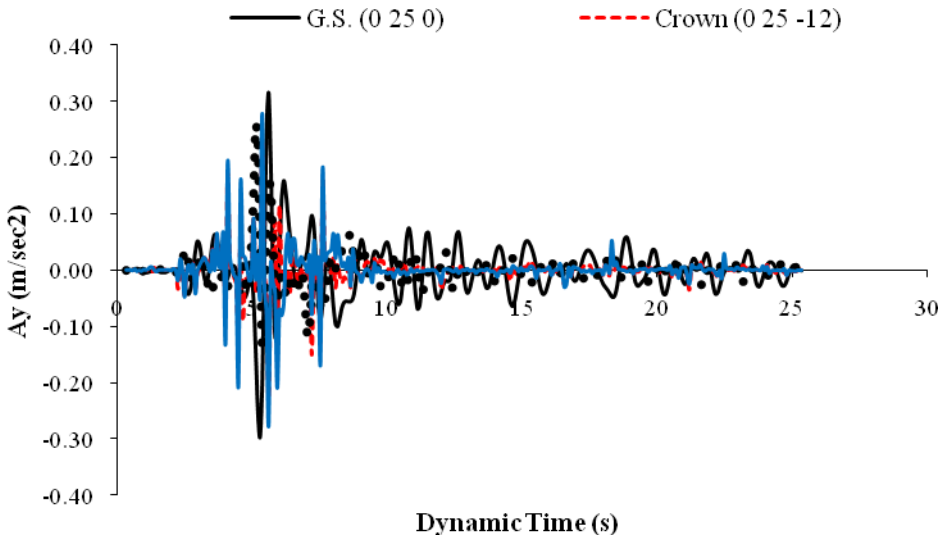

Fig. 17. Time history of longitudinal acceleration at different locations (L component of earthquake) [31].

Table 8. Maximum displacements, *U* (mm) during the earthquake [31].

Points	U_x due to T component of earthquake		U_z due to V component of earthquake	
	2D plane strain analysis	3D analysis	2D plane strain analysis	3D analysis
G.S.	329	201.36	259	227.47
Crown	311	186.77	253	220.45
Invert	301	184.52	251	219.97
S.P. (1)	306	183.7	252	220.00
S.P. (2)	306	183.5	252	222.00

5.8 Remarks

All the displacements in soil-tunnel system were found to be maximum at the ground surface during the earthquake. Higher values of horizontal, vertical and longitudinal displacements were experienced in soil-tunnel system when the system was subjected to T, V, L components of earthquake respectively. Residual forces in RC liners were found to increase only in case when L component of earthquake was applied. In the overall view, 3D analysis yields much subdued dynamic response against the response obtained in 2D plane-strain analysis.

6 Effect of Liquefaction on Lifeline Structures

The factors which affect the liquefaction phenomenon [20, 26] include: i) Type of soil, ii) Shape of soil particles, iii) Grain size distribution, iv) Permeability of Soil, v) Depth of Ground Water Table, vi) Historical Environment, vii) Age of Soil, viii) Confining Pressure, ix) Relative Density, x) Natural Soil Deposits in Water Bodies, xi) Location of drainage and dimensions of deposit, xii) Location of drainage and dimensions of deposit, xiii) Trapped air, and xiv) Presence of Seismic Waves**.** Liquefaction can damage shallow life line structures if they are constructed in strata like poorly saturated soft sandy soils. Life line structures located below the ground water table in liquefiable soils can experience: i) increases in lateral pressure, ii) reduction in lateral passive resistance, iii) sinking or flotation in liquefied soil, iv) lateral displacements, v) permanent settlements, and vi) tension and compression failure after the dissipation of pore water pressure and the consequent consolidation of soil [16].

The seismic response of large underground tunnels constructed in liquefiable soils due to horizontal and vertical components of earthquake was studied by using either the finite difference method or the finite element method by many investigators ([3, 4], [24], [27], and [41]). It was concluded on basis of these studies that – i) Safety of these underground structures against liquefaction damage improves with increase in overburden depth, ii) liquefaction potential of soils was dependent on the overburden depth of tunnel and not on its diameter and thickness, iii) high uplift is mobilized in the tunnel and also the surrounding ground, iv) Forces in tunnels were also found to increase significantly due to earthquake. Moreover, different earthquake loading conditions influence the pore water pressure distribution and subsequently alter the stresses in RC liners. Increasing the loading frequency caused the forces in the tunnel lining and pore water pressure to decrease; although as the loading amplitude decreases, stresses in liners and excessive pore water tend to reduce, v) Deeper tunnels were found to be less vulnerable to liquefaction than the shallow tunnels. The acceleration response at different depths was found to attenuate significantly due to occurrence of soil liquefaction, vi) The increase in amplitude of vertical acceleration increased the liquefaction area, ground surface deformation and uplift of the tunnel structure, but had small influence on internal forces in the tunnel structure. The effect of liquefaction on seismic response of Delhi Metro Underground tunnels was undertaken by [31, 42] and found that the tunnels can suffer damage only if the water table in Delhi area rises to the level of the crown of tunnels, which will not generally happen because the water table will have to rise by at least 10m.

Various life line structures in India are at shallow depth and are susceptible to damage in the event of any major earthquake. So it is important to understand the seismic response of these structures excavated in soils and investigate if they experience any damage due to liquefaction. In this section, an attempt has been made to carry out three dimensional liquefaction analysis of one of the life line structures i.e. Delhi metro underground tunnels using Plaxis 3D software. A set of parametric

studies were also performed by considering different parameters like seismic directions, depth of water table, peak ground acceleration (PGA).

6.1 Analysis of DMRC Tunnel for liquefaction

All other remaining unaltered, the only change is that the depth of overburden above the tunnel is 10.60m and the depth of water table is 17.0m. In-situ unit weight, γ_{bulk} and saturated unit weight, γ_{sat} of Delhi silt were found to be 18 kN/m^3 and 20 kN/m^3 respectively. Damping of soil was taken as 15% for the analysis and the analysis has been carried out for an undrained condition. For this study, engineering properties of alluvium have been adopted from [44] and summarized in Table 9.

Table 9. Properties of soil surrounding the tunnel [44].

Depth	E (MPa)	N_m	*Strength parameters*
0-10	7.54	5	
10-20	18.94	27	*Cohesion,* $c' = 0$
20-30	30.34	49	*Friction angle,* $\varphi' = 35°$
30-40	35.86	59	*Dilation angle,* $\psi' = 5°$
40-50	53.14	92	
50-60	64.54	113	

6.2 Numerical modelling for liquefaction

In order to study the liquefaction response of metro underground tunnels, three dimensional finite element analysis has been carried using Plaxis 3D software. The extent of model, after carrying out sensitivity analysis, has been taken as 200 m x 50 m x 60 in X, Y and Z directions respectively. 10-noded tetrahedral elements with an average size of 6.899 m (< λ, the wave length of the incoming wave) were considered for modelling of soil domain. Segmental RC liners of tunnel were simulated using 6-noded triangular plate bending elements. For RC liners, elastic behavior was considered. No-slip condition has been assumed between tunnel and the surrounding soil medium. Two different material models are taken for modelling the soil. Above the water table hardening soil (HS) model was considered for modelling the soil whereas UBC3D-PLM model was used to model the soil below the water table. As liquefaction occurs only in saturated soils, therefore there is no need to use UBC3D-PLM model in unsaturated soil. The UBC3D-PLM model was first developed by [40]. This model is an extension of the two dimensional UBC-SAND model developed at University of British Colombia.

Some important state variables used in UBC3D-PLM model are tabulated below in Table 10. Pore pressure ratio, *PPR* can show the current status during the calculation procedure and it is given by Eq. (1).

$$PPR = \frac{P_i^{/} - P_c^{/}}{P_i^{/}} \tag{1}$$

where $P^{/}_i$ is the initial effective mean stress and $P^{/}_c$ is the current effective mean stress. Maximum pore pressure ratio (PPR_m) can reveal if the soil liquefies even once during the test. The state variable, r_u gives similar information as *PPR* but instead of the effective mean stress, the vertical effective stress is used as shown in Eq. (2), [40].

$$r_u = \frac{\sigma^{/}_{vertical,i} - \sigma^{/}_{vertical,c}}{\sigma^{/}_{vertical,i}} \tag{2}$$

Parameters defined in UBC3D-PLM model have been calculated in Tables 10 and 11. Some parameters are kept constant for all the layers of soil, and values of these parameters are stated in Table 10, whereas modulus numbers and corrected SPT values vary with depth and are stated in Table 11. Properties of hardening soil material model have been calculated and presented in Tables 12 and 13. Some properties are kept constant with depth of soil and are presented in Table 12 whereas the stiffness varies with depth of soil and values of soil moduli with depth are stated in Table 13. Boundary conditions and earthquake loading was kept same as in section 5.0 (3D analysis).

Table 10. Properties of soil for UBC3D-PLM model [31, 42, 44].

Parameters	Values
Peak friction angle, φ_p (in deg.)	35
Constant volume friction angle, φ_{cv} (in deg.)	29.1
Elastic shear modulus index, *me*	0.5
Elastic bulk modulus index, *ne*	0.5
Plastic shear modulus index, *np*	0.5
Failure ratio, R_f	0.7
Atmospheric pressure, P_A (kPa)	100
Tension cut-off, σ_t (kPa)	0
Densification factor, fac_{hard}	0.45
Post liquefaction factor, fac_{post}	0.2

Table 11. Modulus number and SPT values of soil for UBC3D-PLM model [31, 42, 44].

Depth	N_m	Corrected SPT value, $(N_1)_{60}$	Elastic shear modulus, K_G^e	Elastic bulk modulus, K_B^e	Plastic shear modulus, K_G^P
0-10	5	6	788.2	438.2	185.1
10-20	27	16	1092.6	607.5	939.1
20-30	49	24	1250.5	695.3	2260.9
30-40	59	27	1300.57	723.1	2944.3
40-50	92	37	1444.4	803.1	6032.3
50-60	113	42	1506.7	837.7	8073.55

Table 12. Properties of soil for hardening soil (HS) model [31, 42, 44].

Properties	Symbol	Values
Cohesion	c'	0
Friction angle	φ'	35°
Dilation angle	ψ'	5°
Poisson's ratio for unloading	v	0.2
Reference pressure	P^{ref}	100
K_0 value for normal consolidation	K_0^{nr}	0.426
Failure ratio	R_f	0.7
Power for stress level dependency of stiffness	m	1

Table 13. Moduli values (MPa) for hardening soil (HS) model [31, 42, 44].

Depth	*Initial modulus,* E_i	*Tangent modulus,* E_{50} (=0.65 E_i)	Secant stiffness in SDT test, E_{50}^{ref} (=E_{50})	Tangent stiffness for primary oedometer loading E_{ur}^{ref} (= 3 E_{50}^{ref})	Unloading/reloading stiffness E_{oed}^{ref} (=E_{50}^{ref} / 1.25)
0-10	7.54	4.9	4.9	14.7	3.92
10-20	18.94	12.31	12.31	36.93	9.85
20-30	30.34	19.72	19.72	59.16	15.78
30-40	35.86	23.31	23.31	69.93	18.65
40-50	53.14	34.54	34.54	103.62	27.63
50-60	64.54	41.95	41.95	125.85	33.56

The response obtained after dynamic analysis of DMRC tunnels, when subjected to T component (X-direction) of earthquake, is presented here for discussion

6.3 Displacements

Figure 18 shows the contours of total displacement in soil - tunnel system. Maximum displacement in soil medium is of order of 449.2 mm. The maximum total displacement in the tunnel at the end of T component of earthquake (residual) was found to be 55.37 mm, as shown in Fig. 18.

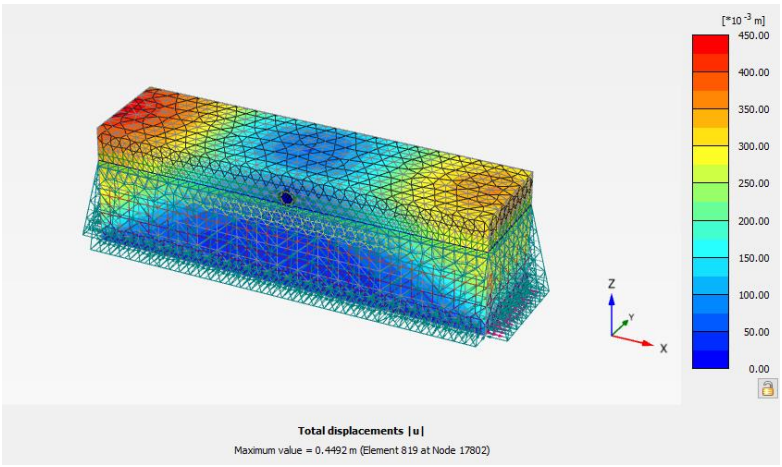

Fig. 18. Total displacement in soil-tunnel system at end of T component of 1999 Chamoli earthquake [31, 42]

Values of static and dynamic displacements in soil mass and RC liners of tunnel have been presented in Table 14. It can be seen that transverse (T) component of earthquake causes significant increase in horizontal (X-direction) and vertical (Z-direction) displacements in soil medium as well as in RC liners. However, Dynamic displacement in longitudinal direction i.e. in Y-direction us much smaller in soil mass and is negligible in RC liners.

Table 14. Static and dynamic displacements is soil-tunnel system(T component of earthquake) [31, 42].

U	Soil medium		RC liners	
	Static displacement	Dynamic displacement	Static displacement	Dynamic displacement
U_x *(mm)*	3.42	183.8	3.584	10.90
U_y *(mm)*	1.153	74.6	0.028	1.98
U_z *(mm)*	5.405	335.4	5.131	54.9

6.4 Liquefaction susceptibility

Liquefaction susceptibility in soil surrounding the tunnel can be checked in terms of pore pressure ratio (*PPR*) and the state variable (r_u). It may be noted that water table

exists at 17.0m below the ground surface. Distribution of maximum pore pressure ratio during the earthquake is presented in Fig. 19.

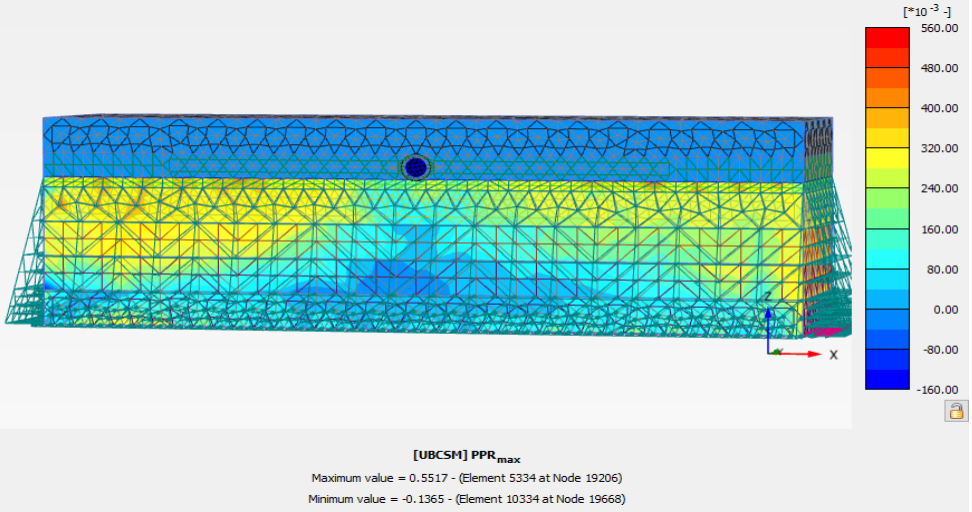

Fig. 19. Maximum pore pressure ratio in soil during the earthquake [31, 42].

It can be seen that maximum value of pore pressure ratio occurs below the tunnel invert. Value of pore pressure ratio (PPR_m) was found to be 0.4 for various points below the invert. Overall maximum value of pore pressure ratio is 0.55 which has been found to occur at points just below the water table (as red color shown in Fig. 19). Pore pressure ratio (*PPR*) after the earthquake was found to be of the order of 0.4 in layer 3 i.e. between depths of 17m to 20m. It was found to be less than 1.0 for both during the earthquake and after the earthquake conditions. Therefore it can be concluded that soil medium surrounding the tunnel is safe against liquefaction. Similarly, susceptibility of liquefaction can be checked in terms of state variable, r_u. It can be found that maximum value of state variable (r_u) is of the order of about 0.65 during the earthquake and it is 0.60 at the end of earthquake. Therefore this parameter also suggests that soil surrounding the tunnel is safe against the liquefaction.

6.5 Parametric study

Effect of seismic directions on liquefaction. Values of liquefaction parameters have been obtained for all three components of earthquake and are presented in Table 15, from which it can be noticed that- i) values of liquefaction parameters are less than unity when seismic waves propagate either in horizontal, X- direction or in vertical, Z- direction; and ii) values of both pore pressure ratio and the state parameter (r_u) are greater than unity when L component (Y-direction) of earthquake was applied along the length of tunnel.

Table 15. Effect of seismic directions on liquefaction [31, 42].

Parameters	T comp. of EQ in X-direction	V comp. of EQ in Z-direction	L comp. of EQ in Y-direction
PPR_m	0.55	0.65	1.244
PPR	0.40	0.42	1.228
r_{um}	0.65	0.67	1.34
r_u	0.60	0.48	1.34

Therefore liquefaction can occur due to the L component of 1999 Chamoli earthquake when seismic waves propagate in the direction parallel to the alignment of tunnel. It can as well be seen from Fig. 20 that liquefaction occurs in layer 3 i.e. at depth between 17 m to 20.0 m.

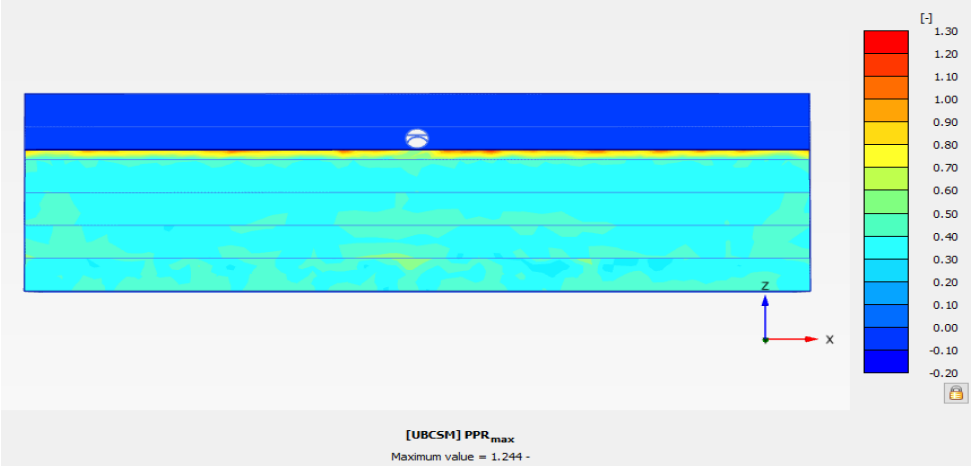

Fig. 20. Pore pressure ratio during L component of 1999 Chamoli earthquake [31, 42].

Effect of depth of water table. Dynamic analysis has therefore been carried out for horizontal, T component (X-direction) of 1999 Chamoli earthquake by considering different depths of water table. Values of liquefaction parameters obtained for different depths of water table ranging between 0.0m to 50m are presented in Table 16. Initially when actual depth of water table was 17m, the soil medium surrounding the tunnel was found to be safe against liquefaction. When depth of water table rises to a level just above the crown of tunnel (h =10m), soil medium surrounding the tunnel was not found to liquefy. It can also be observed that liquefaction occurs in soil mass when water table rises to the ground surface. In that case both pore pressure ratio and state variable (r_u) assume values greater than unity. Therefore, it can be concluded that in present condition (i.e. when water table depth, h =17m), Delhi metro tunnels are safe against liquefaction in the event when seismic waves propagate in the direction of T component of 1999 Chamoli earthquake. However, liquefaction can occur in the event when water table would rise up above to the ground surface.

Table 16. Effect of position of water table on liquefaction [31, 42].

Parameters	Water table depth, h (m)					
	h = 0 m (G.S.)	h = 10m (above the crown)	h = 17m (below the invert)	h = 30m	h = 40m	h = 50m
PPR_m	1.235	0.815	0.55	0.451	0.451	0.45
PPR	1.232	0.845	0.40	0.225	0.125	0.125
r_{um}	1.199	0.852	0.65	0.40	0.36	0.25
r_u	1.199	0.852	0.60	0.32	0.24	0.18

Effect of PGA. In this section, the influence of peak ground acceleration (PGA) on liquefaction has been discussed. For this, depth of water table was retained at 17 m below the ground surface. T component of Chamoli earthquake (PGA = 2.71 m/sec^2) was taken for analysis. The PGA of this earthquake was scaled up to 1.5 m/sec^2, 3.6 m/sec^2, 4.0 m/sec^2 and 5.0 m/sec^2. Values of liquefaction parameters thus obtained are presented in Table 17. It has been found that both pore pressure ratio and state variable (r_u) increase with increase in PGA. But this Delhi site was found to be safe against liquefaction during this earthquake even when PGA was scaled to 4.0 m/sec^2. Soil mass enters the liquefied state only when PGA is scaled beyond up to 5.0 m/sec^2.

Table 17. Effect of PGA on liquefaction [31, 42].

Parameters	PGA = 1.5 m/sec^2	PGA = 2.71 m/sec^2	PGA = 3.6 m/sec^2	PGA = 4.0 m/sec^2	PGA = 5.0 m/sec^2
PPR_m	0.52	0.55	0.61	0.679	1.018
PPR	0.34	0.40	0.50	0.55	0.955
r_{um}	0.36	0.65	0.70	0.74	1.039
r_u	0.36	0.60	0.69	0.74	1.03

6.6 Remarks

Soil medium surrounding the tunnel is safe against liquefaction for T (horizontal) and V (vertical) components of earthquake but liquefaction can occur in case of a seismic event when seismic waves travel in a direction parallel or nearly parallel to the alignment of tunnels. In the present condition when water table depth is at 17m below the ground surface, Delhi metro tunnels are safe against the liquefaction as far as horizontal, T component of Chamoli earthquake is concerned but may become unsafe in situations when water table would rise up to ground surface. Delhi metro tunnels are also safe against liquefaction for this earthquake even when PGA of horizontal, T component of earthquake is scaled up to 4.0 m/sec^2. However, it was found that soil enters into liquefied state when PGA is scaled up to 5.0 m/sec^2.

7 Summary and Conclusions

1. If earthquake data is not available for a particular site, then earthquake record of another similar site should be considered for analysis. Actual earthquake for another site may overestimate or underestimate the response at the proposed site and therefore conversion of actual time history into response spectra time history is very essential.
2. Presence of tunnels modifies the response at the ground surface as compared to that for a free field condition.
3. Tunnels with smaller H/D ratio or with lesser depth of overburden are more prone to damage. Forces in RC liners and settlements in soil-tunnel system are higher in shallow tunnels than in deep tunnels.
4. Three dimensional analysis yields much subdued dynamic response as against the response obtained in 2D plane-strain analysis. 3-D analysis leads to overall reduction in horizontal and vertical displacements and induced acceleration. However, residual forces in RC liners after the earthquake have been found to increase in 3D analysis, the increase due to V component of earthquake being quite significant.
5. Safety of these underground structures against liquefaction damage improves with increase in overburden depth
6. Soil medium surrounding the tunnels is safe against liquefaction for transverse and vertical components of earthquake. However, liquefaction can occur in case of a seismic event when seismic waves travel in a direction parallel or nearly parallel to the alignment of tunnels.
7. In the present condition when water table depth is at 17m below the ground surface, Delhi metro tunnels are safe against the liquefaction as far as T component of 1999 Chamoli earthquake is concerned. However, there can be a cause of concern only if water table rises close to the ground surface.
8. Delhi metro tunnels are also safe against liquefaction for 1999 Chamoli earthquake even when PGA of T component of earthquake (in x-sec. plane) is scaled up to 4.0 m/sec^2. However, it was found that soil enters into liquefied state when PGA is scaled up to 5.0 m/sec^2.

References

1. Abrahamsom, N.A.: Nonstationary Spectral Matching Program RSPMATCH. User's Manual (1992).
2. Atik, L.A., Abrahamson, N.: An improved method for nonstationary spectral matching. Earthquake Spectra, 26(3): 601–617 (2010).
3. Azadi, M., Mohammad, S.M.: Analyses of the effect of seismic behavior of shallow tunnels in liquefiable grounds. Tunneling and Underground Space Tech. 25(5):543–552 (2010).

4. Azadi, M.: The seismic behavior of urban tunnels in soft saturated soils. 12th East Asia-Pacific Conference on Structural Engg. & Construction, Procedia Engg. 14:3069–3075 (2011).
5. Bao, X., Xi, Z., Ye, G., Fu, Y., Su, D.: Numerical analysis on the seismic behavior of a large metro subway tunnel in liquefiable ground. Tunnelling and Underground Space Technology, 66, 91–106 (2017).
6. Basu, B., Gupta, V.K.: Wavelet-based analysis of non-stationary response of a slipping foundation. J. Sound Vibration, 222(4):547–63 (1999).
7. Bolt, B.A., Gregor, N.J.: Synthesized strong ground motions for the seismic condition assessment of the eastern portion of the San Francisco Bay Bridge. Report UCB/EERC-93/12, Earthquake Engineering Research Center, Univ. of California, Berkeley, CA (1993).
8. Chen, Z., Yu, H., Yuan, Y.: Full 3D seismic analysis of a long-distance water conveyance tunnel. Structure and Infrastructure Engineering, 10(1): 128–140 (2014).
9. Chun, L.D., Qi, L.V., Li, D.X., and Chao, M.: Three dimensional seismic response analysis of tunnels and surrounding rock, J. Disaster Prevention and Mitigation Engineering, 02 (2015).
10. Conte, J.P., Peng, B.F.: Fully nonstationary analytical earthquake ground motion model. J. Engg. Mech., ASCE, 123(1): 15–24 (1997).
11. Dowding, C.H., Rozen, A.: Damage to rock tunnels from earthquake shaking. J. Geotechnical Engineering, 2: 175-191 (1978).
12. Fahjan, Y., Ozdemir, Z.: Scaling of earthquake accelerograms for non-linear dynamic analyses to match the earthquake design spectra. 14th World Conference on Earthquake Engineering, Beijing, China (2008).
13. Gasparini, D.A., Vanmarcke, E.H.: Simulated earthquake motion compatible with prescribed response spectra. Massachusetts Institute of Technology, Dept. of Civil Engineering, Constructed Facilities Division, Springfield, Va: Distributed by National Technical Information Service, U.S. Dept. of Commerce (1976).
14. Gupta, I.D., Joshi, R.G.: On synthesizing response spectrum compatible accelerograms. Eur. Earthquake Engg., 7(2): 25–33 (1993).
15. Hashash, Y.A., Hook, J., Schmidt, B., Chiangyao, J.: Seismic design and analysis of underground structures. Tunnelling and Underground Space Technology, 16(4), pp. 247–93, (2001).
16. Hashash, Y. A. Hook, J. Schmidt, B. & Chiangyao, J.: Seismic design and analysis of underground structures. Tunnelling and Underground Space Technology 16(4):247–93 (2011).
17. Ichimura, T., Tanaka, S., Hori, M., Yamamoto, Y., Dobashi, H., Osada, M., Ohbo, N., Yamada, T.: Full three-dimensional seismic response analysis of underground structures with large complex cross sections and two-step analysis method for reducing the computational costs. J. Earthquake and Tsunami, 10(5), pp. 19 (2016).
18. IS 1893 – Part – 1: Criteria for Earthquake Resistant Design of Structures. Bureau of Indian Standards, Manak Bhawan (BIS), New Delhi (2002).
19. Katsanos, E.I., Sextos, A., Manolis, G.D.: Selection of earthquake ground motion records: A state-of-art review from a structural engineering perspective. Soil Dynamics and Earthquake Engineering, 30(4): 157-169 (2010).

20. Kramer, S. L.: Geotechnical Earthquake Engineering", Pub. by Pearson Education Inc. and Dorling Kindersley Pub. Inc. (1996).
21. Kumar A (2006) Software for generation of spectrum compatible time history having same phase as of a given time history. Proceedings of the 8th U.S. National Conference on Earthquake Engineering, San Francisco, California, USA, April 18-22, Paper No. 172.
22. Li, P., Song, E.X.: Three-dimensional numerical analysis for the longitudinal seismic response of tunnels under an asynchronous wave input. Computers and Geotechnics, 63: 229–243 (2015).
23. Lilhanand, K., Tseng, W.S.: Development and application of realistic earthquake time histories comparable with multiple damping design spectra. Proc. Ninth World Conference on Earthquake Engineering, Tokyo-Kyoto, Japan, Vol. 2 (1988).
24. Liu, H., Song, E.: Seismic response of large underground structures in liquefiable soils subjected to horizontal and vertical earthquake excitations. Computers and Geotechnics 32(4):223–244 (2005).
25. Lysmer, J. and Kuhlemeyer, R. L.: Finite dynamic model for infinite media, J. Engineering Mechanics, 95, 859-878 (1969).
26. Prakash, S.: Soil Dynamics, McGraw Hill, New York. Reprinted SP Foundation, Rolla, MO (1981).
27. Salehzadeh, H., Parchami, M.L: Seismic analysis of twin tunnels in liquefiable soils. J. of Transportation Research 2(39): 125-158 (2014).
28. Shrikhande, M., Gupta, V.K.: On generating ensemble of design spectrum-compatible accelerograms. Eur. Earthquake Engg. 3: 49–56 (1996).
29. Shrikhande, M., Gupta, V.K.: On the characterization of the phase spectrum for strong motion synthesis. J. Earthquake Engg. 5(4): 465–82 (2011).
30. Silva, W.J., Lee, K.: WES RASCAL Code for synthesizing earthquake ground motions. In State-of-the-Art for Assessing Earthquake Hazards in the United States, U.S. Army Engineers (1987).
31. Singh M.: Seismic response of shallow metro underground tunnels. Ph.D. thesis, Dept. of Civil Engg., IIT Roorkee, India (2018).
32. Singh, M., Viladkar, M.N., Samadhiya, N.K.: Elasto-plastic analysis of Delhi metro underground tunnels under seismic condition. 16th World Conference on Earthquake Engineering, Santiago, Chile, 9-13, (2017a).
33. Singh, M., Viladkar, M. N. and Samadhiya, N. K. 2017a. Seismic analysis of Delhi metro underground tunnels. Indian Geotechnical Journal, 47(1): 67-83 (2017b).
34. Singh, M., Viladkar, M.N., Samadhiya, N.K.: Three dimensional seismic analysis of metro underground tunnels. Int. Conference on Advances in Construction Materials and Structures, Dept. of Civil Engg., IIT Roorkee (2018).
35. Sliteen, I.., Mroueh, H., Sadek, M.: Three-dimensional modeling of the behavior of shallow tunnel under seismic loading", Laboratory of Civil Engineering and GeoEnvironment (LGCgE), University of Lille 1 – Polytech-Lille, France (2011).
36. Sony, S. : Static and dynamic response of Delhi metro tunnels, Ph.D. Thesis, Dept. of Civil Engg., IIT Delhi, India (2015).
37. Stamos, A.A., and Beskos, D.E.: Dynamic analysis of large 3-D underground structures by the bem. Earthquake Engg. Structural Dynamics, 24(6), 917–34 (1995).

38. Stamos, A.A., Beskos, D.E.: 3-D seismic response analysis of long lined tunnels in half-space. Soil Dynamics Earthquake Engg. 15(2): 111–118 (1996).
39. Trifunac, M.D., Udwadia, F.E., Brady, A.G.: High frequency errors and instrument corrections of strong-motion accelerogram. Earthquake Energy Res. Lab EERL, 71-05, CALTECH., Pasadena, California (1971).
40. Tsegaye, A.: Plaxis liquefaction model. External report. Plaxis knowledge base, http://www.plaxis.nl (2010).
41. Unutmaz, B.: 3D liquefaction assessment of soils surrounding circular tunnels. Tunneling and Underground SpaceTechnology. 40:85–94 (2014).
42 Viladkar, M. N. Singh, M., Samadhiya, N. K.: Liquefaction analysis of metro underground tunnels, 7 Int. Conf. on Earthquake Geotechnical Engineering, Rome, Italy (2019).
43. Wong, H.L., Trifunac, M.D.: Generation of artificial strong motion accelerograms. Earthquake Engg. and Struct. Dynamics, 7: 509–27 (1979).
44. Yadav, H. R.: Geotechnical evaluation of Delhi metro tunnels, Ph.D. Thesis, Dept. of Civil Engg., IIT Delhi, India (2005).
45. Yu, H., Yuan, Y., and Bobet, A.: Seismic analysis of long tunnels: A review of simplified and unified methods, Underground Space, 2, 73–87 (2017).
46. Yu, H., Yuan, Y., Chen, Z., Yu, G., and Gu, Y.: Full 3D numerical simulation method and its application to seismic response analysis of water-conveyance tunnel, Computational Structural Engineering, pp: 349-358 (2009).